FLOW VISUALIZATIONS IN A SHORT-DURATION SUPER-/HYPERSONIC WIND TUNNEL

Paul Krogmann, Erich Schülein

Keywords: *Schlieren or shadowgraphy, oil film interferometry, liquid crystal coatings*

Abstract

The paper describes the application of flow visualisation procedures in the DLR Goettingen Ludwieg Tube Facility RWG. A brief introduction of the experimental facility and its main features will be presented. The techniques which are described in use in the facility are Schlieren or shadowgraph visualisation of the flow fields, oil film interferometry to obtain skin friction data in complex flow field regions on a model and liquid crystal coatings which are used for visualisation of the global thermal load distribution on a model.

1. Introduction

The resolution of experimental data on flow effects in aerodynamic investigations often is limited by the number of data acquisition channels and the space needed for the sensors to be placed on sometimes fairly small wind tunnel models. Especially for high supersonic or even hypersonic flow conditions the experimental facilities, for economic reasons, are designed and built as short duration run time facilities. In addition to measured flow properties visualisation of the flow field about the model or flow effects at the model wall can contribute valuable information to the understanding and interpretation of the experimental results.

In the following a special type of super/ hypersonic wind tunnel facility and a number of flow visualisation methods, routinely used in it, will be described.

Additionally, some more sophisticated methods which have been exploratorily applied will be mentioned.

Author(s): *Paul Krogmann, Erich Schülein*
German Aerospace Center, DLR
Institute of Fluid Mechanics,
Goettingen, Germany

2. The DLR Ludwieg Tube Facility

The basic idea of a low cost tube wind tunnel for high speed and high Reynolds number flow originally was developed by Professor **Ludwieg** some forty years ago. He proposed to use a long tube as pressure reservoir which is closed at one end and to the other end a quick-opening device, a gate valve or a diaphragm, is attached, followed by a super-sonic nozzle, test section and a dump tank [1]. The flow is started by an unsteady expansion wave which propagates through the pressurized test gas along the tube after opening the gate valve or rupturing the diaphragm. Behind the expansion wave test gas flows out of the tube at constant stagnation conditions through nozzle and test section into the dump tank, as long as the expansion wave needs to travel to the closed tube end where it is reflected and finally approaches again at the nozzle throat. Then a new expansion wave generates undergoing the same procedure, as long as the pressure ratio suffices the desired flow establishment.

To Ludwieg`s honor, this principle in anglican literature, later, commonly was called **"Ludwieg Tube".**

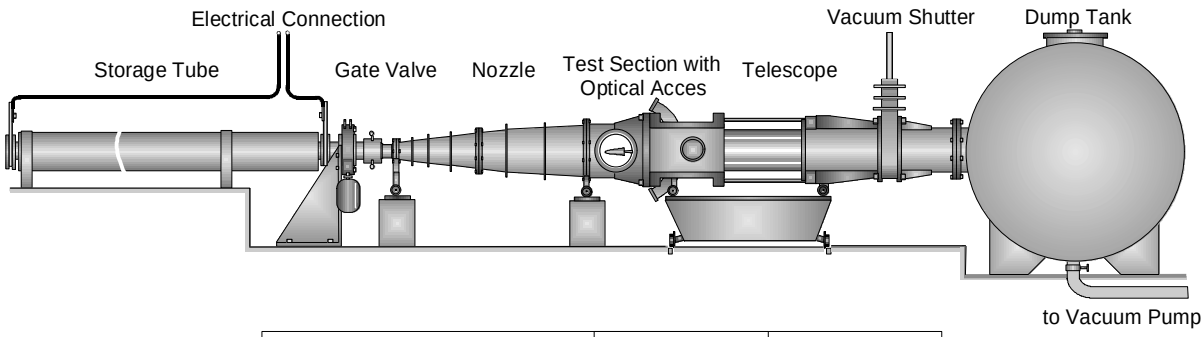

Performance	Tube A	Tube B
Max. Stag. Pressure, bar	15	40
Max. Stag. Temperature, °C	20	400
Mach Number	2.79 to 4.65	5.0 to 6.9
Unit Reynolds Number, 10^6 m^{-1}	5 to 60	5 to 50
Run Time, s	0.4	0.3
Test Section	0.5 x 0.5 m²	∅ 0.5 m

Figure 1: The DLR Ludwieg Tube facility (RWG) at Göttingen

After verifying this operational principle by a small pilot tunnel, the present facility was built with three test-legs for Mach numbers from three up to eleven [2], named in german language "**R**ohr-**W**indkanal **G**öttingen" (RWG).

In RWG normally only the first expansion wave travel time is utilized, then the valve is closed again and up to 70 % of the initial charge pressure is saved in the tube. Thus, the pumping time is considerably reduced.

Since the expansion wave propagates at about the speed of sound in the test gas (air), the run time of the tunnel is determined by twice the tube length and the speed of sound. Here, the tubes are built 80 m long, giving a run time, depending on the charge temperature, of ≈0.3 to 0.4 seconds. **Figure 1** shows the general arrangement of the wind tunnel test-leg B together with main features and achievable flow conditions for the two test-legs (the third one is presently not operational).

Before a test the charge tube is pressurized to the desired value and for Mach numbers beyond five the test gas is pre-heated by heating the tube wall electrically over the whole tube length sufficiently in order to avoid test gas condensation during the strong expansion in the nozzle. Since the tubes can be charged each up to maximum design pressure, very high Reynolds numbers can be achieved. The Reynolds number can be varied independently either by pressure or to a certain amount by temperature variation alone. Since no disturbance-producing devices, as pressure regulating valve, heater, grids etc., are located upstream of the nozzle, the incoming flow to the nozzle is "clean" and a high quality flow in the test section is achieved.

3. Schlieren and Shadowgram Visualization

Observations of the flow field about a wind tunnel model during testing can reveal particular flow features which might not detected in quantitative measurements because of limited instrumentation on the model. During experiments in RWG generally (if possible) the flow field about the model is observed by taking photographs of the schlieren (density gradients) image or the shadowgram (second derivative of the density).

Figure 2 shows schlieren images of the flow field around the shuttle orbiter at Mach seven at an incidence of 45° viewed from the side and from the top [3]. Especially in the top view, **Figure 2 b,** the complexity of the flow around the model is demonstrated. The three-dimensional bow shock system interacts with the leading edge of the model wing which causes increased heat loads at the impingement location which cannot be observed in the side view image which is

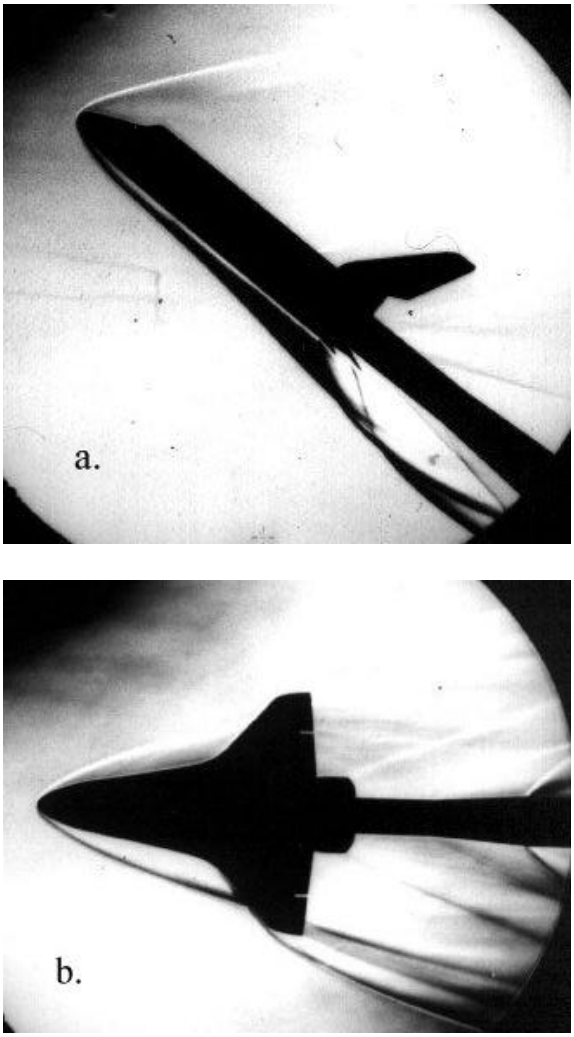

Figure 2: Schlieren images of the shuttle orbiter at M_∞=6.8, α = 45°, a) side view, b) top view

normally observed in wind tunnel testing. Thus, the qualitative schlieren image can give precious aid for the placement of instrumentation on a model to be used for heat flux measurements, for example.

Within an ESA sponsored contract work on validation experiments for numerical codes boundary layer profile measurements and local skin friction measurements by a newly applied interferometric method were carried out in RWG at Mach five on a flat plate flow where the turbulent boundary layer was disturbed by an impinging oblique shock wave of different strengths [4]. Here, the schlieren observations not only served for visualization of the shock system, but also for visualization of the effect of the impinging shock wave on the boundary layer.

The flow field over the flat plate is shown as shadowgram in **Figure 3.** The shock generator is a flat plate at incidence mounted above the plate, such that for each incidence (shock strength) of the shock generator the impingement location was always at the same position on the plate. The pressure rise due to the shock is transmitted upstream over the subsonic part of the boundary layer and causes the boundary layer to separate, well distinguishable in the image.

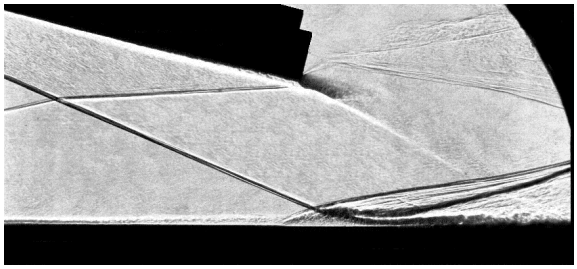

Figure 3: Oblique shock (generator angle Θ=14°) impinging on flat plate boundary layer at M_∞ = 5 , $Re_\infty = 4 * 10^7\ m^{-1}$

4. Global Interferometry Skin Friction

The same test set-up was used for quantitative determination of local skin friction on the flat plate by an interferometric method which was applied for the first time in the short duration run time Ludwieg Tube facility [12].

For the application of this technique the surface of the model has to be highly reflective at the desired measurement location which is covered by a thin film of oil with appropriate viscosity which has to be known for data reduction. The desired location is illuminated by coherent laser light. The reflected light rays from the surface and the upper surface of the oil film interfere and produce an image of

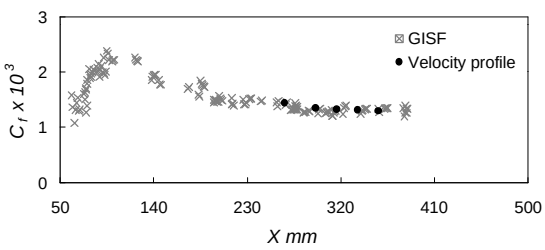

Figure 4: Local skin friction coefficients on a flat plate determined from B.L. profile measurements and by Global Interferometry Skin Friction (GISF)

interference fringes. Caused by the local skin friction the thickness of the oil film varies, causing a variation of the fringe pattern which is used for determining the local skin friction coefficient.

Figure 4 shows the skin friction distribution along the flat plate as obtained from boundary layer profile measurements with a pitot probe and by the non-intrusive oil film interferometry. It is seen that at about X = 100 mm the transition from laminar to turbulent is completed and the skin friction coefficients decrease slowly in downstream direction.

This interferometric technique presently is used in an investigation of the three-dimensional flow behind a vertical fin mounted on a flat surface representing a generic model of a fuselage with a fin [5].

In **Figure 5a** the general test arrangement is shown schematically and **Figure 5c** presents a typical fringe pattern obtained by oil film interferometry where lines of separation (marked "S" and "S'") and re-attachment (marked "R") can be clearly distinguished. **Figure 5b** depicts schematically the surface skin friction directions (developed from Fig. 5b). of the highly three-dimensional flow behind the fin.

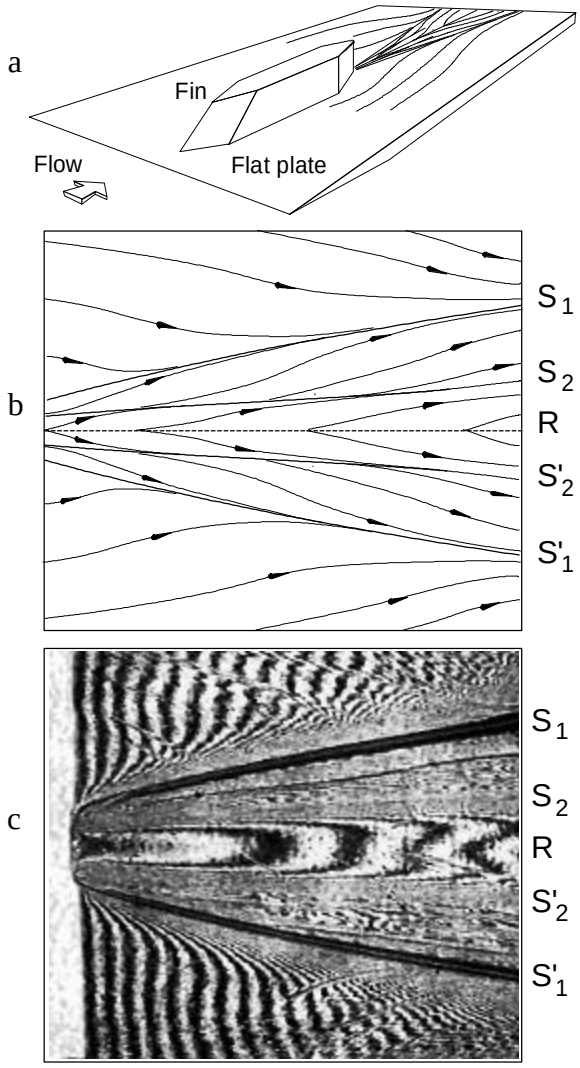

Figure 5: Flow in the wake of a vertical fin

5. Surface Oil Flow Pattern

Because of the relative short run time of the Ludwieg Tube, the application of surface oil flow visualization was considered to be not possible for a long time, until oil with appropriate viscosity was found.

The oil is mixed with the white titanium oxide in a certain ratio which has to be determined experimentally to be optimum.

The oil-titanium - mixture is applied to the blackened model surface, either as droplets with a sponge or by a brush. The image of the oil film has to be taken during run by photograph or continuously by a CCD - camera, since the surface oil flow pattern is destroyed to a certain extent by flow break-down at the end of a test run. The oil mixture during run is washed in the direction of the local skin friction leaving a pattern on the model surface, depending on local flow conditions. At locations of flow separation, where the skin friction tends to zero, oil mixture is accumulated and at regions of high friction it may be washed away completely.

During re-entry of the Space Shuttle from the very first orbital mission the deflections of body flap and elevons hardly managed to

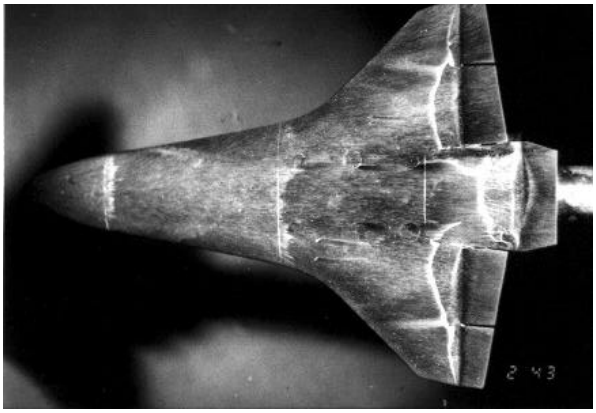

Figure 6: Oil flow pattern on windward shuttle surface, $M_\infty = 7$, $\alpha = 45°$

trim the vehicle to a stable flight attitude. The reason for this might have been boundary layer separation upstream of the control elements, as is evident in **Figure 6.** Upstream of the deflected body flap and elevons regions of separated flow are visible which may reduce the effectiveness of the control surfaces seriously.

Within the **E**uropean **S**pace **A**gency (ESA) HERMES re-entry vehicle program for manned space transportation the Ludwieg Tube facility, due to its large Reynolds number variation range, was selected to perform heat flux and pressure distribution measurements on a configuration representing the windward center-line of the HERMES vehicle at an incidence of α = 30° with deflected body flap. The experimental results should be used as reference data for validation of numerical codes. In order to faciltate the numerical computations the HERMES contour was approximated by an hyperboloid with a conical flare extension representing the deflected body flap [7][8][9][10]. Thus, the problem, in reality being three-dimensional, was reduced for the computations to a two-dimensional one. In addition to the quantitative pressure and heat flux measurements, different flow visualization techniques were applied for verification purposes. **Figure 7** depicts a surface oil flow pattern obtained at Mach 6.8 and at a unit Reynolds number of $Re_\infty = 10^7\ m^{-1}$.

A large region upstream of the flare (body flap hinge line) is seen to be influenced by flow separation, caused by the pressure increase due to the flare. The flow re-attaches on the flare, detectable by the less accumulated oil mixture traces.

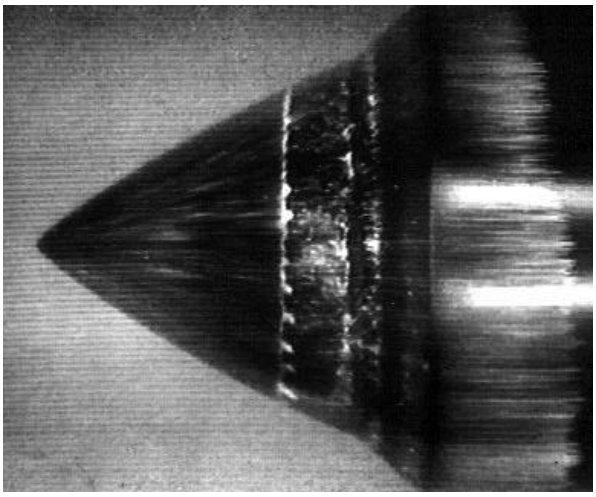

Figure 7: Oil flow pattern on a hyperboloid/flare at $M_\infty = 6.8$, $Re_\infty = 10^7\ m^{-1}$, $\alpha = 0°$

6. Liquid Crystal Heat Flux Pattern

Especially for the design of the thermal protection system of spaceflight vehicles re-entering the atmosphere the absolute value of local heat load and especially the location of maximum heat load has to be known as precisely as possible.

The "Liquid Crystal technique" (LC) offers a simple means for obtaining a quick overview of the heat load distribution even on complicated three-dimensional models.

The thermosensitive Liquid Crystals change their colour depending on temperature. They are commercially available for specified temperature ranges. Below range they appear transparent on a black surface, change colour from red over yellow, green to blue with increasing surface temperature, and seem transparent again if the surface temperature is beyond the range of the LC.

In applying this technique the blackened surface of the model of low conductive material is coated with a thin layer of LC of desired temperature range. After drying of the coating the model is ready for testing. Since the colour changes are reversible, the model can be used for multiple tests, as long as the coating is not destroyed.

Figure 8 shows a Liquid Crystal image of the hyperboloid/flare model at the same flow conditions as in figure 7.

At the nose of the model the surface temperature, due to the high heat flux, is beyond the range of the LC coating, therefore, the model here appears black. Further downstream the local heat flux decreases and the surface temperature is within the range of the LC coating, indicated by the colour change. At the location of separation the local heat flux is very low so that the temperature is below the active LC range, thus, the model again appears black. After re-attachment of the flow on the flare the local heat flux increases dramatically

causing the surface temperature to rise beyond the LC range.

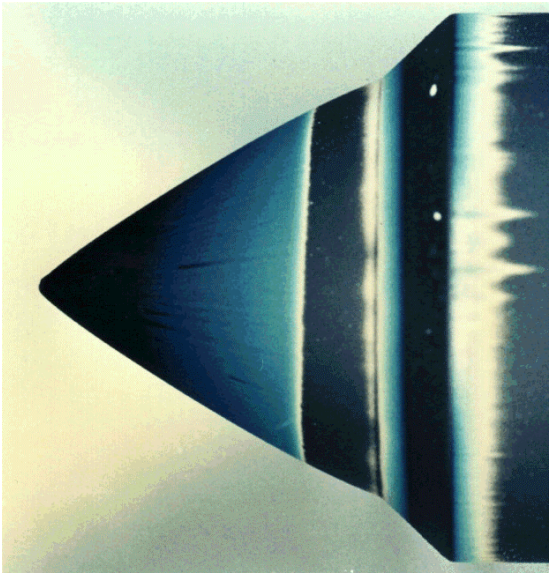

Figure 8: LC heat flux pattern on a hyperboloid/flare at M_∞=6.8, $Re_\infty = 10^7\ m^{-1}$, $\alpha = 0°$

On three-dimensional models the flow may become extremely complicated by shock-boundary layer interactions, vortices emanating from edges and flow separations. **Figure 9** shows a LC image of the upper side of the SÄNGER configuration at Mach 6.8 and at small angle of attack which was investigated within a "single stage to orbit" technology program [11].
The orbiter was supposed to be carried piggy-back by a carrier airplane up to an altitude of about 40 km where the orbiter would be released to start, rocket-propelled, as single stage into orbit. The carrier airplane then would land again conventionally on an ordinary airport runway.

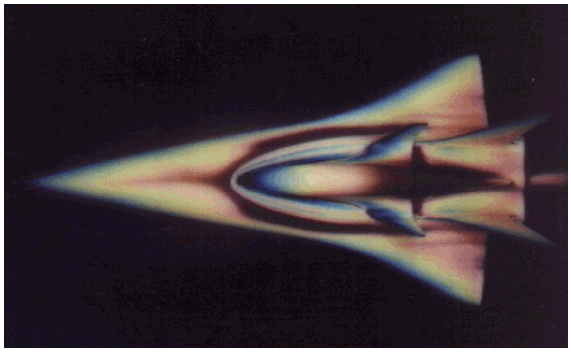

Figure 9: Liquid Crystal image of the SÄNGER single stage to orbit configuration, $M_\infty = 6.8$, $\alpha = 2°$

The LC image reveals the complex flow conditions existing on the model. High heat loads at the leading edges of the wing and fins and at the nose of the orbiter are denoted by the blue colour. The shock at the orbiter nose causes the flow to separate, indicated by black colour of the surface. In the edges formed by the orbiter and the carrier surface develop vortices whose traces can be detected as blue lines at the sides of the orbiter.

7. Different Means

So far all flow visualization techniques routinely applied in RWG investigations at super-/hypersonic speeds have been described. They are easily applied and do not need a complicated optical test set-up.
However, different more sophisticated methods which need a high power laser light source and corresponding high quality receiving optics have also been used.
The LIF technique (**L**aser **I**nduced **F**luorescence) has been applied successfully in the investigation of the flow field in the stagnation region of an ellipsoid at Mach 6.8. For this the test gas (normally air) was mixed with a few percent of nitric oxide (NO). The NO- molecules in the test region were exited by a thin EXIMER - Laser light sheet to emit light which then can be analysed to obtain information about flow properties in the region of examination [12][13].
Further, a holographic interferometer set-up has been used to study unsteady shock-induced disturbances on a transonic profile in a modified test section of tunnel A [14]. A similar test set-up was used at higher Mach number (M = 5) to investigate the shock-shock interaction region in front of a cylinder where the cylinder bow shock interacts with an impinging oblique shock wave [14][15]. The holographic interferometer image was filmed during tunnel run with a high speed film camera (2000 frames/second). Thus, unsteady flow effects could be analysed.
Laser Doppler **V**elocimeter (LDV) and **P**article **I**mage **V**elocimetry (PIV) are considered to be **not** suitable for this type of

wind tunnel because of "seeding" problems due to the relatively high supply pressure used and the strong acceleration within the nozzle inlet and during the rapid expansion along the nozzle.

8. Concluding Remarks

The flow visualization techniques routinely used in aerothermodynamic investigations in the DLR Ludwieg Tube facility at Göttingen, including a description of the operational characteristics of the wind tunnel principle, have been presented.
Despite of the short run time of the wind tunnel of a few tenth of a second, nearly all visualization techniques have proven to be well suited for application and are used frequently in RWG investigations.

9. References

[1] **Ludwieg, H., D**er Rohrwindkanal. Zeitschrift für Flugwissenschaften ZFW, vol. 3, Nr. 7, pp. 206 -216, (1955)

[2] **Ludwieg, H., Hottner, Th., Grauer-Carstensen, H.,** Der Rohrwindkanal der Aerodynamischen Versuchsanstalt Göttingen. Jahrbuch der DGLR 1969, pp. 52 - 58, (1970)

[3] **Krogmann, P., Schneider, W.,** Six-component force measurements on a shuttle configuration at Mach 7 in the Ludwieg Tube B. DFVLR IB 222- C 22, (1987)

[4] **Schülein, E., Krogmann, P., Stanewsky, E.,** Documentation of two-dimensional impinging shock/turbulent boundary layer interaction flow. DLR IB 223 -96 A 49 (1996)

[5] **Schülein, E.,** Work in progress. To be published (1998)

[6] **Krogmann, P., Schöler, H.,** Windkanalversuche zur Sichtbarmachung des Strömungsfeldes und der Wärmeflußverteilung an der SÄNGER - Konfiguration bei Mach 6.8. DFVLR IB 222- 88 C 18, (1988)

[7] **Krogmann, P.,** Hyperboloid/flare experiments at Mach 6.8 in RWG. DLR IB 223 94 - C 44 (1994) ESA/CNES H - NT - 0 - 2074 - DLR (1994)

[8] **Krogmann, P.,** Calibration and Validation measurements in the Ludwieg Tube Tunnel B (RWG). DLR IB 223 - 95 C 28, (1995) ESA/CNES HT-TR-E-1-301-DLRG, (1995)

[9] **Krogmann, P.,** Hyperboloid/flare investigations at Mach 6.8. First Europe-US high speed flow field database workshop, part II, November 12 - 14, 1997, Naples, Italy

[10] **Krogmann, P., Schwane, R.,** Synthesis of test case T 1 - 97: Hyperboloid/flare. Proceedings of First Europe-US high speed flow field database workshop, part II. To be published, (1998)

[11] **Krogmann, P., Schöler, H.,** Windkanalversuche zur Sichtbarmachung des Strömungsfeldes und der Wärmeflußverteilung an der SÄNGER - Konfiguration bei Mach 6.8. DFVLR IB 222 - 88 C 18, (1988)

[12] **Schülein, E., Koch, S., Rosemann, H.,** Skin friction measurement and transition detectingtechniques fr the Ludwieg Tubes at DLR. RTO/AGARD Fluid Dynamic Measurement Technology, September 22 - 25, 1997, Seattle, USA, pp. 23-1 - 23-9

[13] **Bütefisch, K.-A., Krogmann, P. et al.,** Measurement techniques for hypersonic flows. Lecture Series von Karman Institute for Fluid Dynamics, 28. 5. - 1. 6. 1990, Rhode-St. Genèse, Belgium

[14] **Bütefisch, K.-A., Krogmann, P.,** Application of **L**aser **I**nduced **F**luorescence and Rayleigh scattering to supersonic flows in a jet and in a wind tunnel. Proceedings EUROMECH 260, 5. - 7. 9. 1990, Poitiers, France

[15] **Basler, D.,** Experimentelle Untersuchung der Ausbreitung stoßinduzierter Störungen an transsonischen Profilen. Dissertation, Universität Göttingen, (1987)

[16] **Knauer, A.,** Aufbau eines holographischen Interferometers. Studienarbeit, TU Hannover, (1992)

[17] **Knauer, A.,** Experimentelle Untersuchung der Soß-Stoß- Wechselwirkung bei Überschallgeschwindigkeiten mit Hilfe eines holographischen Interferometers. Diplomarbeit, TU Hannover (1993)